

## P2Y purinoceptors mediate ATP-induced changes in intracellular calcium and amylase release in acinar cells of mouse parotid glands

Kasumi MORIGUCHI-MORI<sup>1, 2</sup>, Hironori HIGASHIO<sup>3</sup>, Kanako ISOBE<sup>1, 2</sup>, Miho KUMAGAI<sup>2</sup>, Kana SASAKI<sup>1</sup>, Yoh-ichi SATOH<sup>1, 4</sup>, Akiyoshi KUJI<sup>2</sup>, and Tomoyuki SAINO<sup>1</sup>

<sup>1</sup>Department of Anatomy (Cell Biology), <sup>3</sup>Department of Chemistry, Center for Liberal Arts and Sciences, and <sup>4</sup>Department of Medical Education, Iwate Medical University, 2-1-1 Nishitokuta, Yahaba-cho, Shiwa-gun, Iwate 028-3694, Japan and <sup>2</sup>Division of Special Care Dentistry, Department of Developmental Oral Health Science, School of Dentistry, Iwate Medical University, 1-3-27 Chuodori, Morioka, Iwate 020-8505, Japan

(Received 7 December 2015; and accepted 15 December 2015)

### ABSTRACT

Adenosine 5'-triphosphate (ATP) can act as an extracellular signal that regulates various cellular functions. The present study aimed to determine which purinoceptors play a role in ATP-induced changes in intracellular  $\text{Ca}^{2+}$  ( $[\text{Ca}^{2+}]_i$ ) and amylase secretion in mouse parotid glands. ATP induced a steep increase in  $[\text{Ca}^{2+}]_i$  in acinar cells. The removal of extracellular  $\text{Ca}^{2+}$  or the use of  $\text{Ca}^{2+}$  channel blockers slightly inhibited this increase. Inhibition of PLC $\gamma$  by U73122 and of IP $_3$  by xestospongin C did not completely block this increase. The purinoceptor antagonists suramin and reactive blue-2 strongly inhibited the ATP-induced changes in  $[\text{Ca}^{2+}]_i$ . 2-MeSATP induced a strong increase in  $[\text{Ca}^{2+}]_i$ , while Bz-ATP induced a small  $[\text{Ca}^{2+}]_i$  increase, and UTP and  $\alpha, \beta$ -MeATP had no effect. The potency order of ATP analogs (2-MeSATP > ATP >> UTP) suggested that P2Y $_1$  and P2Y $_{12}$  play a significant role in the cellular response to ATP. RT-PCR revealed that P2X $_{2,4,7}$  and P2Y $_{1,2,10,12,14}$  were expressed in acinar cells.  $\text{Ca}^{2+}$ -dependent exocytotic secretion of amylase was detected in parotid glands. These findings indicated that ATP activates P2Y receptors more than P2X receptors at low concentrations. Thus, P2Y receptors were found to be the main receptors involved in  $\text{Ca}^{2+}$ -related cell homeostasis and amylase secretion in mouse parotid glands.

Salivary glands, including parotid glands, are exocrine glands composed of multiple secretory end pieces called “acini,” which secrete saliva into the oral cavity via a system of branched ductal cells (28). The acinar cells secrete primary saliva, which is a plasma-like, isotonic fluid. The ductal cells reabsorb  $\text{Na}^+$  and  $\text{Cl}^-$  from primary saliva and excrete  $\text{K}^+$  and  $\text{HCO}_3^-$  into the final saliva. The salivary secretion from acini and modification of the electrolytes in

ducts are regulated by an increase in the intracellular  $\text{Ca}^{2+}$  concentration ( $[\text{Ca}^{2+}]_i$ ) through the activation of  $\text{Ca}^{2+}$ -dependent ion channels and transporters (39). The regulation of salivary secretions is under neural control, and also activation of the sensory nerves in acini and ducts initiates an afferent pathway leading to the central nervous system. This pathway activates an efferent pathway that stimulates parasympathetic and sympathetic nerves that innervate the parotid gland (46).

Adenosine 5'-triphosphate (ATP) can be found in extracellular spaces where it functions as a neurotransmitter or a co-transmitter that is released from nerve endings (11, 13, 23, 26, 60). ATP is also known to leak from injured or stimulated cells (14, 37). In addition, it has been proposed that ATP is involved in specific extracellular signaling actions, thus playing

---

Address correspondence to: Tomoyuki Saino, M.D., Ph.D.

Laboratory of Cell Biology, Department of Anatomy, Iwate Medical University, 2-1-1 Nishitokuta, Yahaba-cho, Shiwa-gun, Iwate 028-3694, Japan

Tel: +81-19-651-5111, Fax: +81-19-908-8006

E-mail: tsaino@iwate-med.ac.jp

a role in the regulation of a variety of functions (e.g., development, proliferation, differentiation, and secretion) in a number of tissues (2, 54). The role of nucleotides as extracellular cell signaling molecules is well established (11, 15, 16). Purinergic receptors are important for the induction of the ATP signaling function. These receptors can be divided into two main categories: P1 purinoceptors (adenosine receptors) and P2 purinoceptors (ATP receptors) (12, 47). Stimulation of P2 purinoceptors by ATP leads to either a rapid excitatory response via the activation of ionotropic P2X purinoceptors, which are ligand-gated, non-selective cation channels, or to metabotropic responses, which are mediated by the G protein-coupled receptor family of P2Y purinoceptors (1, 15, 21, 24, 32). Seven P2X receptors (ionotropic receptors, P2X<sub>1-7</sub>) and eight P2Y receptors (metabotropic receptors, P2Y<sub>1,2,4,6,10,12-14</sub>) have been identified in mammals (17, 41).

Both P2X and P2Y receptors are highly expressed in secretory epithelia and are involved in the modulation of fluid secretion (32, 42, 53). Recent studies have demonstrated that the P2X<sub>7</sub> receptor is expressed in the mouse parotid gland (8, 34, 43, 48). Li *et al.* reported that ATP can induce an increase in [Ca<sup>2+</sup>]<sub>i</sub> via the P2X<sub>7</sub> receptor (34). Noteworthy, much higher concentrations (EC<sub>50</sub> ≈ 300 μM) of a P2X<sub>7</sub> agonist than those of ATP are required for these effects (22). In rat parotid gland acinar cells, extracellular ATP at concentrations > 50 μM dose-dependently increases [Ca<sup>2+</sup>]<sub>i</sub> via activation of P2Z (P2X<sub>7</sub>) purinoceptors. The response seemed to involve the activation of a P2 purinoceptor subtype different from P2Z because maximum responses were induced by much lower concentrations (< 0.25 mM) of ATP than those (> 1 mM) required to produce maximum activation of Ca<sup>2+</sup> entry (59). The exocytotic action of nerve endings can result in the accumulation of micromolar concentrations of extracellular ATP (26). Recently, Baldini *et al.* showed the involvement of the P2X<sub>7</sub> receptor–inflammasome–caspase-1–IL-18 axis in the development of primary Sjögren's syndrome exocrinopathy (4). In lacrimal glands, a P2Y<sub>2</sub> agonist was found to improve ocular surface health in a rat dry eye model based on the induction of increased tear fluid secretion and the release of glycoprotein-containing moieties from goblet cells (25). However, there are few data on P2Y receptors of parotid glands (3, 45, 56). Therefore, it is necessary to understand whether the effect of ATP on parotid glands is mediated by metabotropic P2Y receptors under physiological conditions.

The aim of the present study was to determine the

contribution of P2Y as well as P2X purinoceptors to ATP-induced changes in [Ca<sup>2+</sup>]<sub>i</sub> and to estimate salivary amylase activity in parotid gland acinar cells. For this purpose, we examined the [Ca<sup>2+</sup>]<sub>i</sub> dynamics in mouse semi-intact parotid gland acinar cells that retained their essential cellular structure. We recently succeeded in showing that ATP participates in a variety of signaling activities in different tissues (29, 36, 50). In case of lacrimal glands, the response of acinar cells to ATP is mediated by P2Y (especially, P2Y<sub>1</sub>) as well as by P2X purinoceptors (29). The present study focused on the identification of the types of purinoceptors that are present in acinar cells of mouse parotid glands and mediate the effect of ATP on the [Ca<sup>2+</sup>]<sub>i</sub> levels in these cells.

## MATERIALS AND METHODS

*Preparation of mouse glandular acini.* Protocols and all animal experiments were approved by and conducted under the authority of the Iwate Medical University Institutional Animal Care and Use Committee. Adult female ICR mice (12–18 weeks old, body weight 30–38 g) were used. The mice were sacrificed with carbon dioxide gas, and then perfused via the left cardiac ventricle with Ringer's solution (147 mM NaCl, 4 mM KCl, and 2.25 mM CaCl<sub>2</sub>) at room temperature. The parotid glands were removed and placed in Hepes-buffered Ringer's solution (HR) containing 118 mM NaCl, 4.7 mM KCl, 1.25 mM CaCl<sub>2</sub>, 1.13 mM MgCl<sub>2</sub>, 1 mM NaH<sub>2</sub>PO<sub>4</sub>, 5.5 mM D-glucose, MEM amino acids solution (Gibco, Grand Island, NY, USA), 0.2% bovine serum albumin (Sigma, St. Louis, MO, USA), and 10 mM Hepes, and the pH was adjusted to pH 7.4 with NaOH.

The parotid glands were trimmed of excessive connective tissues and digested with collagenase (100 U/mL; Elastin Products, Owensville, MO, USA) in HR buffer for 1 h at 37°C. Enzyme digestion was conducted with constant agitation (~200 cycles/min) in a rotary shaker under an atmosphere of 100% O<sub>2</sub> that was achieved by gassing at 15-min intervals. After digestion, the glands were washed twice and centrifuged at 800 ×g for 2 min at room temperature between washes. The pellet was resuspended in 15 mL of HR buffer. The suspension was filtered through a Nitex screen (100 mesh/inch). Then, the glands were washed twice and centrifuged at 800 ×g for 2 min at room temperature between washes. The final pellet was resuspended in 3 mL of HR buffer.

*Intracellular Ca<sup>2+</sup> imaging.* The specimens were transferred into HR buffer containing 5 μM Ca<sup>2+</sup>-sensitive

Indo-1/AM dye and were incubated for 1 h at 37°C. After incubation, in order to measure  $[Ca^{2+}]_i$ , parotid gland acinar cells were placed on coverslips coated with Cell-Tak<sup>®</sup> (a nontoxic adhesive reagent; Collaborative Biomedical Products, Bedford, MA, USA) in modified Sykus-Moor chambers and were then continuously perfused with HR buffer containing selected stimulants. Indo-1 is a ratiometric dye that is excited by ultraviolet light and is used for semi-quantitative determination of  $[Ca^{2+}]_i$ . The emission maximum of Indo-1 shifts from 475 nm in  $Ca^{2+}$ -free medium to 400 nm when the dye solution is saturated with  $Ca^{2+}$ . The ratio of the emission intensity at a wavelength shorter than 440 nm to that at a wavelength longer than 440 nm can be used to estimate  $[Ca^{2+}]_i$ ; a higher ratio indicates higher  $[Ca^{2+}]_i$ . Artifacts including photobleaching and dye leakage can be eliminated using this ratiometric dye.

A real-time confocal microscope (RCM/Ab; a modified version of a Nikon model RCM-8000, Tokyo, Japan) was used to measure cellular  $[Ca^{2+}]_i$  changes. Additionally, we measured  $[Ca^{2+}]_i$  changes in specific, restricted areas of the cell (~1  $\mu m^2$  spot size). Indo-1-loaded cells were exposed to an ultraviolet beam (351 nm). An inverted microscope was equipped with an argon-ion laser (TE-300, Nikon), and the fluorescence emission was passed through a water-immersion objective lens (Nikon C Apo 40 $\times$ , N.A. 1.15) to a pinhole diaphragm. Using this system, the acquisition time per image frame was 1/30 s. Digital images were composed of 512  $\times$  480 pixels with a resolution of 8 bits/pixel and were immediately stored on high-speed hard disks. Fluorescence intensity was displayed as pseudocolor with 256 colors; red represents high  $[Ca^{2+}]_i$ , and purple and blue low  $[Ca^{2+}]_i$ .

**Treatments.** The  $[Ca^{2+}]_i$  dynamics of acini were examined in a perfusion chamber as quickly as possible after the dye-loading procedure. After perfusion with the standard HR solution for a few min at room temperature, intact parotid glands were selected and examined under the microscope. Specimens were continuously perfused with HR solution containing the following agonists and/or antagonists: adenosine (50  $\mu M$ ), adenosine 5'-monophosphate (AMP, 50  $\mu M$ ), adenosine 5'-diphosphate (ADP, 50  $\mu M$ ),  $\alpha,\beta$ -methyleadenosine 5'-triphosphate ( $\alpha,\beta$ -MeATP, 50  $\mu M$ ; a typical agonist of P2X<sub>1,3</sub>), uridine triphosphate (UTP, 50  $\mu M$ ; an agonist of P2Y<sub>2,4,6</sub>), 2-methylthioadenosine-5'-O-triphosphate (2-MeSATP, 50  $\mu M$ ; a P2Y receptor agonist), 2'(3')-O-(4-benzoylbenzoyl)-adenosine 5'-triphosphate (BzATP, 50  $\mu M$ ; an agonist

of P2X<sub>7</sub>), U73122 (5  $\mu M$ ; an inhibitor of phospholipase C), diltiazem (50  $\mu M$ ; an L-type  $Ca^{2+}$  channel blocker), and carbachol (CCh, 10  $\mu M$ ; a cholinergic agonist), all from Sigma; adenosine 5'-triphosphate (ATP, 50  $\mu M$ ) from Kohjin Life Sciences (Tokyo, Japan); suramin (50  $\mu M$ ; an antagonist of P2 purinoceptors) and reactive blue-2 (RB-2, 50  $\mu M$ ; an antagonist of P2Y purinoceptors), both from Research Biochemicals International (Natick, MA, USA); and GdCl<sub>3</sub> (100  $\mu M$ ; a nonspecific cation channel blocker), xestospongine C (2  $\mu M$ ; a selective and membrane-permeable inhibitor of IP<sub>3</sub> receptors) and tetrodotoxin (TTX, 2  $\mu M$ ; a sodium channel blocker) from Wako (Osaka, Japan). To compare ATP-induced  $[Ca^{2+}]_i$  dynamics with those induced by a cholinergic (muscarinic) stimulus, we perfused the parotid glands with HR containing CCh.

**RNA extraction and reverse transcription polymerase chain reaction (RT-PCR).** Parotid glands from mice were digested with collagenase in HR buffer as described above. Total RNA was extracted using the RNeasy Micro Kit (Qiagen, Hilden, Germany) according to the manufacturer's instructions. Isolated RNA was subjected to RT-PCR that was performed with a thermal cycler (PC-701; ASTEC, Fukuoka, Japan) using the ReverTra Ace- $\alpha$ <sup>®</sup> (TOYOBO, Osaka, Japan). The primers used in this study were those reported by Ohtani *et al.* (44) for P2X purinoceptors and by Zhang *et al.* (63) for P2Y purinoceptors; the sequences are listed in Table 1. The thermal cycling protocol was as follows: 42°C for 10 min, 94°C for 1 min, followed by 35 cycles of 94°C for 45 s, 60°C (or the appropriate primer-specific annealing temperature, see Table 1) for 30 s, and 72°C for 2 min, and final extension at 72°C for 10 min. The PCR products were electrophoresed in 2% agarose gels and stained with ethidium bromide. Images of the gels were captured using a Polaroid MP4 land camera (Polaroid, Minneapolis, MN, USA). Each RT-PCR was repeated in three independent experiments.

**Amylase activity.** Parotid gland acinar cells were preincubated in 1 mL of HR buffer at 37°C for 5 min and stimulated with 500  $\mu M$  ATP, 500  $\mu M$  2-MeSATP, or 2  $\mu M$  A23187 for 1 h. Preincubated cells without stimulation (incubated in HR buffer for 1 h) were used as controls. The cell suspensions were chilled on ice for 5 min to terminate secretion and centrifuged at 137  $\times g$  for 2 min at 4°C. The amylase activity in aliquots of the supernatants was assessed using an  $\alpha$ -Amylase Assay Kit (Kikkoman Corp., Tokyo, Japan) according to the manufacturer's in-

**Table 1** Primers used for RT-PCR of the mRNA of P2 receptors

Gene		Sequence 5'-3'	Position	Accession Code	Amplicon
P2X1	F	TGGGTGGGTGTTGTCTATG	305	NM008771	310 bp
	R	GTTGCCTGTGCGAATACCTT	614		
P2X2	F	AACAGCATCCACTATCCCAAG	684	NM153400	339 bp
	R	GGTGGTGCCGTTTATCTTGT	1022		
P2X3	F	AGGTGTCCCATCTCCTTTTTG	3029	NM145526	307 bp
	R	AGAGTTGAGTTGAGGGAGGAGA	3335		
P2X4	F	TCTCACTCGGTCTCCACTCC	1359	NM011026	339 bp
	R	AACAGCACACCAGAAATCCA	1697		
P2X5	F	GGGTTTCGTGTTGTCTCTGTTT	89	NM033321	455 bp
	R	GTAGAGTTCCCCACCCGTAGA	543		
P2X6	F	ACCAACTTCCTCGTGACACC	475	NM011028	448 bp
	R	GCAGCTGGAAGGAGTACTGG	1003		
P2X7	F	ACCCTGTCTACTTTGGCTTG	1181	NM011027	329 bp
	R	GAGTCGTGGAGAGATAGGGACA	1509		
P2Y1	F	TTTTGTAAACATGGTCACAAGACATCCC	1804	NM008772	381 bp
	R	AGTGGCCACGTCACGGTTTT	2184		
P2Y2	F	GCTCCGTCATGCTGGGTCT	1071	NM008773	360 bp
	R	CTCGGGCAAAGCGGACAA	1430		
P2Y4	F	ACTGGAACATAAGATGGTGCTCCT	141	NM020621	559 bp
	R	GCAGATGCCCATGTAGCGGT	699		
P2Y6	F	AGCCCACCATCCTGTCT	941	NM183168	323 bp
	R	GGCCGAGTGCCTTTGTAG	1263		
P2Y10	F	CTTGACATGCATTAGCCTTCAG	650	NM172435	578 bp
	R	GAGCTTCCATGACGAGATAGTTG	1249		
P2Y12	F	CCATTGACCGCTACCTGA	730	NM027571	334 bp
	R	GGAACCTTTGGCTGAACCC	1063		
P2Y13	F	CTATGAGACGATGTATGTGGGTAT	382	NM028808	379 bp
	R	CTTGTGCCTGCTGTCCTTAC	760		
P2Y14	F	CCTTGCTGTCCCAAACAT	976	NM133200	337 bp
	R	ACCTTCCGTCTGACTCTTT	1312		
GAPDH	F	AGCCTCGTCCCGTAGACAAA	36	BC083079	379 bp
	R	GAGATGATGACCCTTTTGGC	414		

F, forward primer; R, reverse primer. The primers are from Ohtani *et al.* (44) and Zhang *et al.* (63). P2Y10 primers were designed using the web-based tool "Primer3." All primers were assessed for specificity using BLAST searches (<http://www.ncbi.nlm.nih.gov/blast>).

structions. The absorbance at 400 nm was measured using a spectrophotometer (UV-1600; Shimadzu, Kyoto, Japan).

**Statistical analysis.** The quantitative results are presented as the mean  $\pm$  SD of three independent determinations. Student's *t*-test was used to compare treated to untreated cells;  $P < 0.05$  was considered significant.

## RESULTS

**Effects of ATP and ATP analogs on  $[Ca^{2+}]_i$  dynamics**  
We analyzed the effects of ATP and ATP analogs on  $[Ca^{2+}]_i$  dynamics in mouse parotid gland acinar cells. As we did not aim to include the myoepithelial cells

that cover the acini in this study, we set the focal plane on the equatorial planes of the acini and placed the regions of interest (ROIs) for the time course of  $[Ca^{2+}]_i$  dynamics on acinar cells. No spontaneous  $[Ca^{2+}]_i$  changes were observed in the acinar cells of the parotid glands. Exposure of the parotid glands to extracellular ATP led to an increase in  $[Ca^{2+}]_i$  in some acinar cells (number of experiments;  $n = 12$ ) (Figs. 1a–d). Spatial analysis of  $[Ca^{2+}]_i$  changes in acini indicated that both ATP- and CCh-induced  $[Ca^{2+}]_i$  increases started in the central region of the acini (Fig. 2a–l). ATP-induced  $[Ca^{2+}]_i$  changes showed a biphasic behavior; the first step involved a steep phase of rapidly increasing  $[Ca^{2+}]_i$ , followed by a second weak plateau phase step. The second, sustained increase in  $[Ca^{2+}]_i$  was more prolonged in aci-

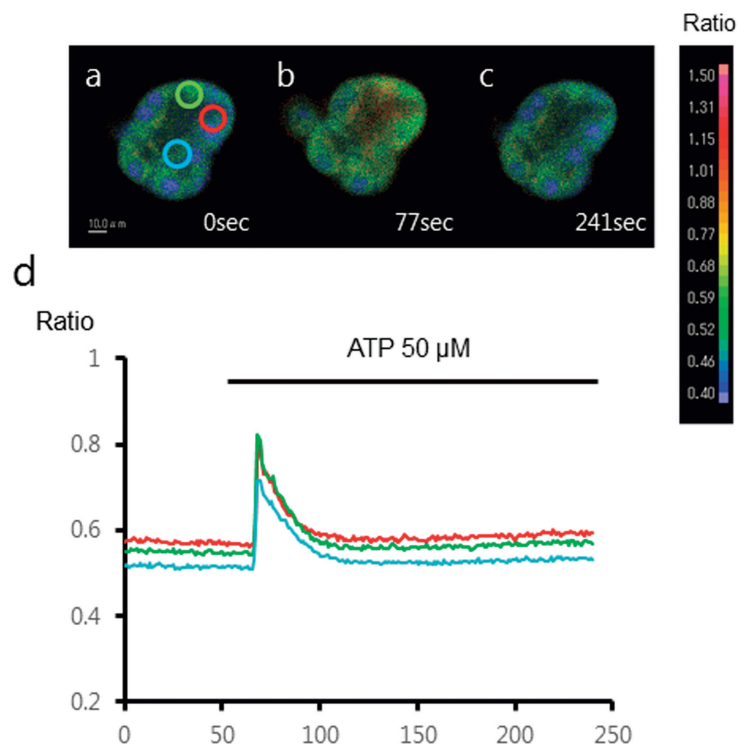


**Fig. 1** Spatiotemporal changes in  $[Ca^{2+}]_i$  in acinar cells during ATP stimulation. Changes in  $[Ca^{2+}]_i$  are indicated as pseudo-colors (a–c). Color scale bar:  $[Ca^{2+}]_i$  was calculated based on the ratio of dye fluorescence intensities at different wavelengths. d: Time course of ATP-induced changes in  $[Ca^{2+}]_i$  in specific areas (i.e., regions of interest; ROIs) of parotid gland acinar cells ( $\sim 1 \mu m^2$  in size).

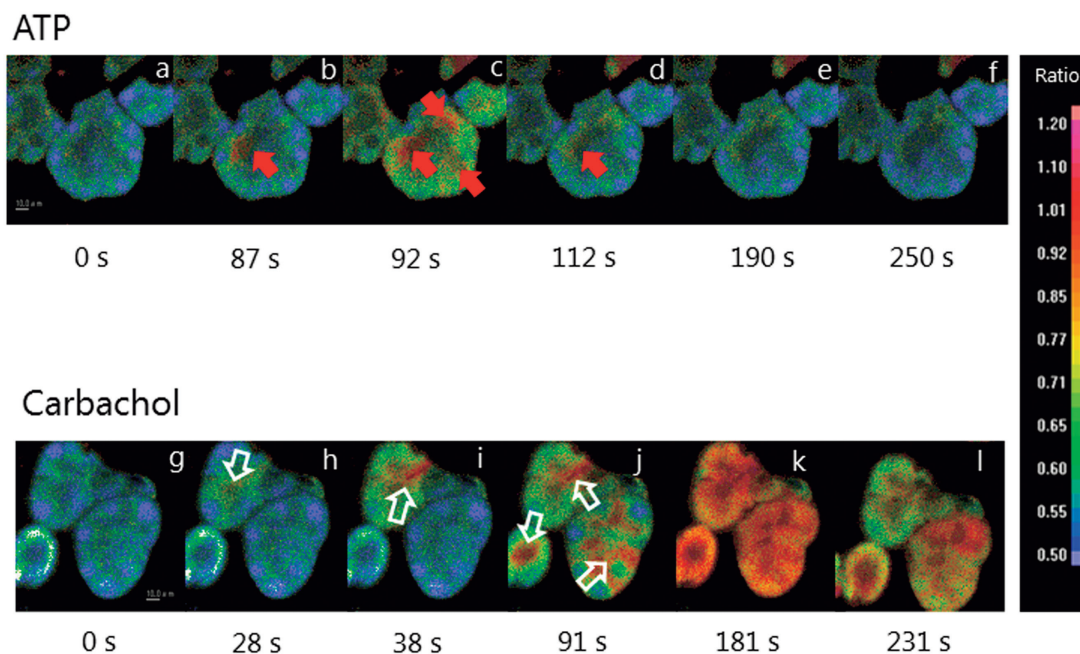


**Fig. 2** Spatial analysis of  $[Ca^{2+}]_i$  changes induced by ATP and CCh. Pseudocolor images of ATP (50  $\mu M$ ; a–f) and CCh (10  $\mu M$ ; g–l)-induced  $[Ca^{2+}]_i$  changes in parotid gland acinar cells. The ATP-induced  $[Ca^{2+}]_i$  increase started from the central regions of the acini (full red arrow). Similarly, the CCh-induced  $[Ca^{2+}]_i$  increase was initiated from the central regions of the acini (open white arrow).

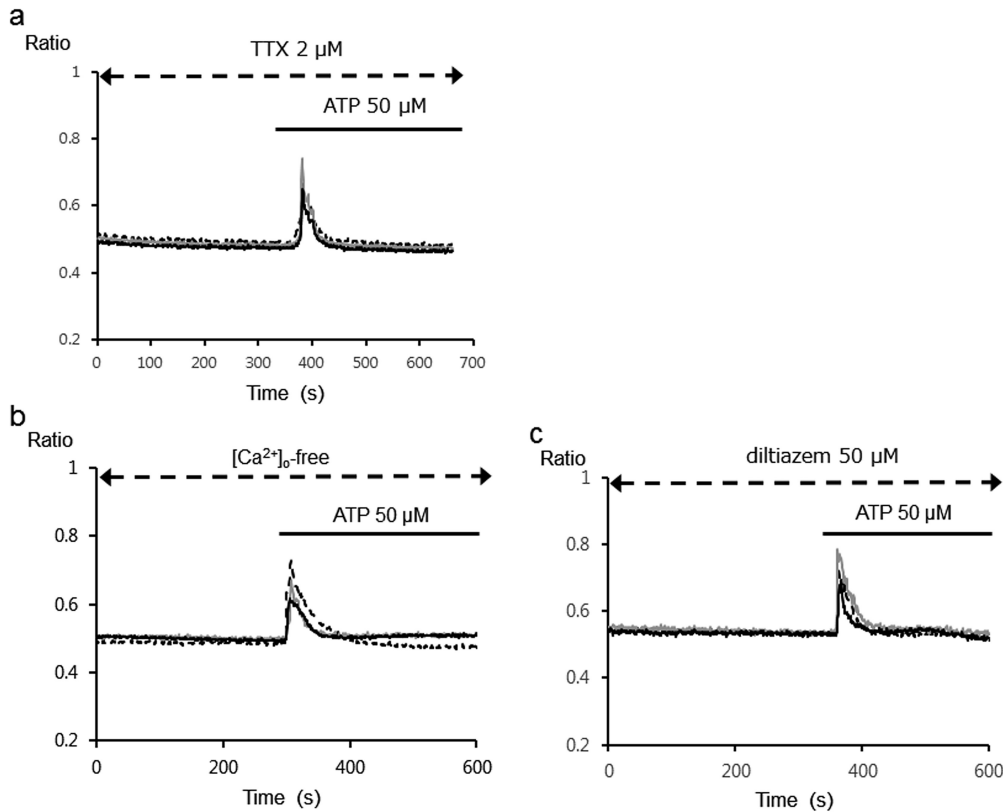


**Fig. 3** Ion channels are not completely responsible for ATP-induced  $[Ca^{2+}]_i$  changes. The time course of  $[Ca^{2+}]_i$  changes induced by ATP in specific areas of parotid gland acinar cells ( $\sim 1 \mu m^2$  in size) was analyzed as described for Fig. 1. ATP ( $50 \mu M$ )-induced  $[Ca^{2+}]_i$  increases are not inhibited by TTX (**a**). Either extracellular  $Ca^{2+}$ -free conditions ( $[Ca^{2+}]_o$ -free) (**b**) or treatment with  $50 \mu M$  diltiazem (**c**) slightly inhibited ATP-induced  $[Ca^{2+}]_i$  increases. Three ROIs were set for these analyses.

ni stimulated with CCh than in those stimulated with ATP. Thus, even after cessation of CCh stimulation, the  $[Ca^{2+}]_i$  level remained elevated for several minutes and then gradually declined (data not shown). The size and shape of the acini showed little changes during ATP and CCh stimulation.

Next, we attempted to determine whether pharmacological blockade of neuronal excitability prevents the ATP-induced response. Inhibition of  $Na^+$  inward currents was achieved by exposure to the sodium channel blocker TTX ( $2 \mu M$ ). TTX did not completely inhibit ATP-induced  $[Ca^{2+}]_i$  dynamics ( $n = 7$ ) (Fig. 3a), suggesting that ATP-induced  $Ca^{2+}$  influx in parotid acinar cells might not depend on nerve-mediated membrane depolarization correlated with fluxes of  $Na^+$  and  $K^+$  ions. Mechanisms that control  $Ca^{2+}$  uptake into intracellular stores or effusion of  $Ca^{2+}$  into the extracellular space contribute to  $Ca^{2+}$  homeostasis and the shape of  $Ca^{2+}$  transients (6, 31). To analyze the mechanism by which ATP induces changes in  $[Ca^{2+}]_i$ , we further investigated if ion channels such as the ionotropic purinoceptors were complete-

ly responsible for ATP-induced changes in  $[Ca^{2+}]_i$ . ATP-induced  $[Ca^{2+}]_i$  changes in parotid gland acinar cells were not completely inhibited in the absence of extracellular  $Ca^{2+}$  ( $[Ca^{2+}]_o$ ) ( $n = 10$ ) (Fig. 3b). Treatment of acinar cells with diltiazem ( $50 \mu M$ ), an L-type  $Ca^{2+}$  channel blocker, also did not completely inhibit ATP-induced  $[Ca^{2+}]_i$  increases ( $n = 10$ ) (Fig. 3c). Furthermore, no complete inhibition of ATP-induced  $[Ca^{2+}]_i$  increases was observed following treatment with  $Gd^{3+}$  ( $100 \mu M$ ) ( $n = 10$ ), a nonspecific cation channel blocker (data not shown). These data suggested that receptors other than ion channels might participate in the activity of ATP. In general, metabotropic receptors are G-protein-linked, and stimulation of G protein activates phospholipase C (PLC), which cleaves membrane-bound phosphatidylinositol-bisphosphate to generate inositol-triphosphate ( $IP_3$ ) and diacylglycerol.  $IP_3$  subsequently causes  $Ca^{2+}$  mobilization from internal stores (7). To determine if this mechanism of  $Ca^{2+}$  mobilization was involved in the ATP-dependent  $[Ca^{2+}]_i$  increase, the effect of U73122, an inhibitor of PLC, was analyzed. U73122

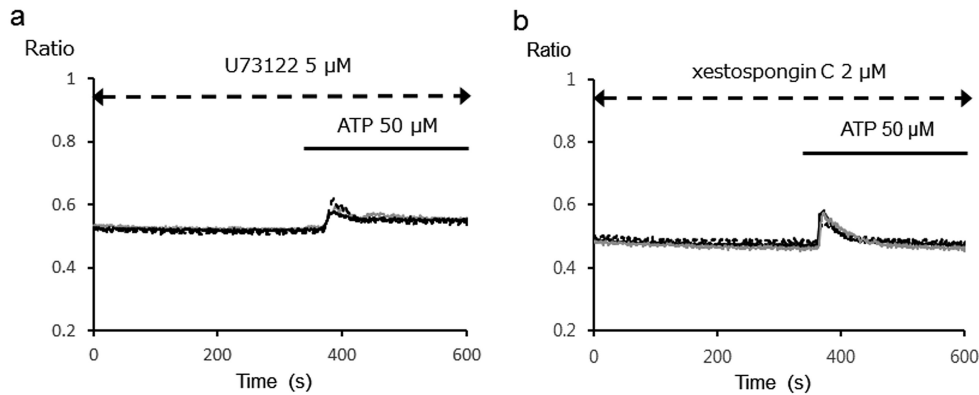


**Fig. 4** A role of mobilization of  $Ca^{2+}$  from intracellular  $Ca^{2+}$  stores in ATP-induced  $[Ca^{2+}]_i$  changes. **a:** ATP (50  $\mu$ M) induced only a slight  $[Ca^{2+}]_i$  increase in the cells after blocking of phospholipase C by treatment with U73122 (5  $\mu$ M). **b:** Treatment with the  $IP_3$  receptor antagonist, xestospongine C (2  $\mu$ M), partially inhibited ATP-induced  $[Ca^{2+}]_i$  increases. Three ROIs were set for these analyses.

(5  $\mu$ M) inhibited the ATP-induced increase in  $[Ca^{2+}]_i$  ( $n = 9$ ) (Fig. 4a) and xestospongine C (2  $\mu$ M; a selective and membrane-permeable inhibitor of  $IP_3$  receptors) considerably blocked this increase ( $n = 8$ ) (Fig. 4b). Thus, both  $Ca^{2+}$  influx from extracellular spaces and  $IP_3$ -dependent  $Ca^{2+}$  mobilization from intracellular  $Ca^{2+}$  stores were induced by ATP stimulation, and intracellular mobilization of  $Ca^{2+}$  may be more significant than  $Ca^{2+}$  influx in the ATP-induced response.

Next, we studied the involvement of P1 and P2 purinoceptors in the effect of ATP and its analogs on parotid gland acinar cells using specific agonists and antagonists of these receptors. P1 purinoceptors are more responsive to adenosine and AMP than to ADP and ATP, and, conversely, P2 purinoceptors are more responsive to ADP and ATP than to adenosine and AMP (12). In the present study, AMP (50  $\mu$ M) failed to induce a  $[Ca^{2+}]_i$  increase ( $n = 9$ ) (Fig. 5a). Adenosine (50  $\mu$ M) had a similar effect ( $n = 8$ ) (data not shown). Consistent with this observation, suramin (a non-selective P2 purinoceptor antagonist; 50  $\mu$ M) completely inhibited the ATP-induced  $[Ca^{2+}]_i$  increase ( $n = 8$ ) (Fig. 5b). These data indicated that ATP-induced responses are mediated by P2, but not P1 receptors. It has been reported that parotid glands express some ionotropic P2X purinoceptors (8, 10, 18, 33, 34); however, there are few studies of metabotropic P2Y receptors in the parotid gland (3, 45, 56). Therefore, we analyzed the potential contribution of P2 receptor subtypes to ATP-induced  $[Ca^{2+}]_i$  increases in parotid gland acinar cells using receptor-specific agonists and antagonists. Reactive blue-2 (RB-2; 50  $\mu$ M), an antagonist of P2Y purinoceptors, strongly inhibited the ATP-induced increase in  $[Ca^{2+}]_i$  ( $n = 9$ ) (Fig. 5c). The P2Y receptor agonist 2-MeSATP (50  $\mu$ M)

induced large changes in  $[Ca^{2+}]_i$  dynamics in these cells ( $n = 9$ ) (Fig. 6a), whereas the P2X<sub>7</sub> agonist BzATP (50  $\mu$ M) induced a small change in  $[Ca^{2+}]_i$  ( $n = 8$ ) (Fig. 6b). However, the P2Y<sub>2,4,6</sub> agonist UTP (50  $\mu$ M) and the P2X<sub>1,3</sub> agonist  $\alpha,\beta$ -MeATP (50  $\mu$ M) had no effect ( $n = 9$ ,  $n = 8$ , respectively) (Figs. 6c and 6d). Therefore, we conclude that P2Y purinoceptors play a major role in ATP-induced changes in  $[Ca^{2+}]_i$  dynamics, although  $Ca^{2+}$  influx via P2X purinoceptors could also occur.

#### *Amylase secretion*

The involvement of ATP in amylase secretion was investigated. Acini were preincubated with various concentrations of ATP for 1 h. Dose-dependent release of amylase was observed (Fig. 7a). We checked the increase in amylase activity using 500  $\mu$ M ATP and 500  $\mu$ M 2-MeSATP. Both agonists significantly induced amylase secretion after 1 h of incubation (Fig. 7b). To determine whether  $[Ca^{2+}]_i$  is involved in the amylase secretion, the effect of a 1-h treatment with the  $Ca^{2+}$  ionophore A23187 (2  $\mu$ M) was investigated. Amylase secretion was significantly stimulated by A23187 (Fig. 7b). These results suggested that ATP induces an increase in  $[Ca^{2+}]_i$ , which stimulates amylase secretion.

#### *P2 receptor mRNA expression in parotid gland acinar cells*

Finally, we assessed the expression of P2 receptor mRNAs in parotid gland acinar cells using RT-PCR. Receptor expression levels were graded from (–), where the PCR product was not detectable by ethidium bromide staining of an agarose gel, to (++) , where a very strong band was detected in the gel

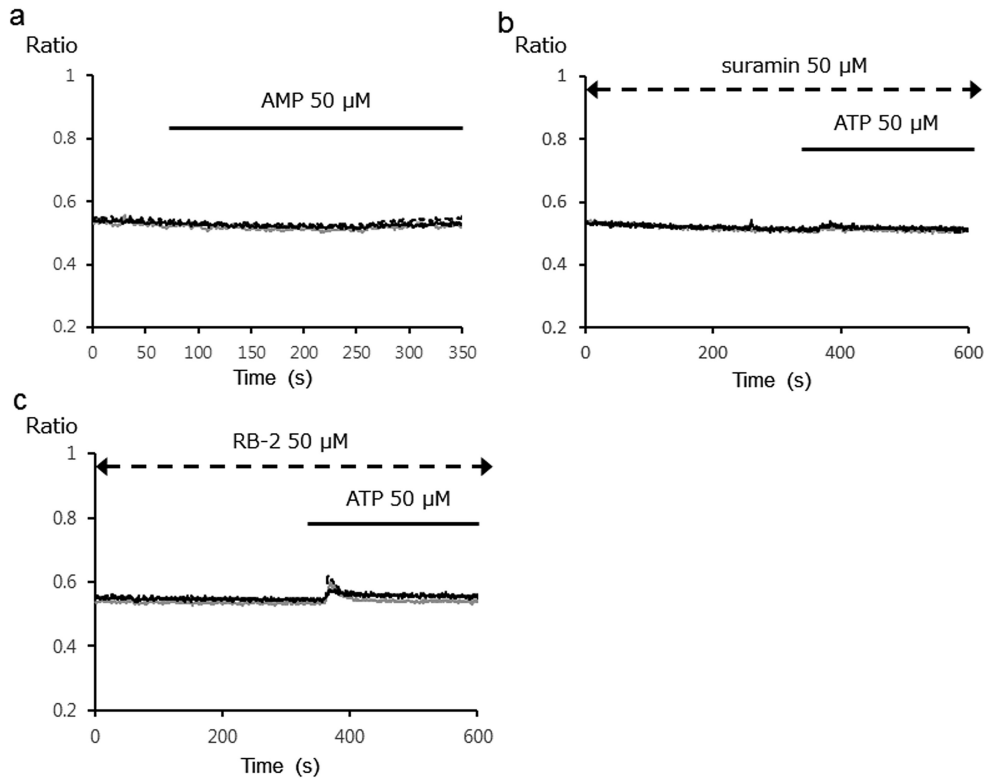


**Fig. 5** Effect of P1 and P2 purinoceptor agonists/antagonists on  $[Ca^{2+}]_i$  changes induced over time by ATP. Cells were stimulated with 50  $\mu$ M ATP. **a:** The P1 agonist AMP (50  $\mu$ M) had no effect on  $[Ca^{2+}]_i$  dynamics. **b:** The P2 antagonist suramin (50  $\mu$ M) completely inhibited ATP-induced  $[Ca^{2+}]_i$  increases. **c:** The P2Y antagonist reactive blue-2 (RB-2; 50  $\mu$ M) blocked ATP-induced  $[Ca^{2+}]_i$  increases. Three ROIs were set for these analyses.

(Fig. 8). P2X<sub>2,4,7</sub> and P2Y<sub>1,2,10,12,14</sub> were expressed in mouse parotid gland acinar cells (Fig. 8).

## DISCUSSION

ATP plays an important role in amylase secretion from salivary glands. Agonist-induced increases in  $[Ca^{2+}]_i$  are involved in initiating saliva secretion, the primary physiological function of parotid gland acinar cells (39). Most of the previous studies have reported that these cells are stimulated via P2X receptors, especially the P2X<sub>7</sub> receptor. Based on the data of the present study, we propose that metabotropic P2Y receptors also play a significant role in ATP stimulation of parotid gland acinar cells. This study demonstrated that  $Ca^{2+}$  mobilization from intracellular  $Ca^{2+}$  stores was induced by extracellular ATP, suggesting the presence of metabotropic receptors that are activated by ATP. Experiments using U73122 or xestospongine C indicated that the ATP-induced responses were mediated mainly by IP<sub>3</sub> receptor-mediated  $Ca^{2+}$  mobilization. The results of stimulation/inhibition with ATP analogs and antago-

nists indicated that parotid gland acinar cells also express metabotropic P2Y receptors. According to the review of Burnstock (16), the agonist potency order of 2-MeSATP > ATP >>> UTP =  $\alpha, \beta$ -MeATP indicated that P2Y<sub>1</sub> and P2Y<sub>12</sub> were the main receptors for mediation of ATP-induced responses.

P2X<sub>7</sub> has been previously studied in parotid gland acinar cells (8, 33, 34, 40, 43, 48) and in lacrimal glands (19, 20, 27, 43). Casas-Pruneda *et al.* reported a functional interaction between P2X<sub>7</sub> and P2X<sub>4</sub> receptors in epithelial cells from salivary glands, and this functional interaction could be important in generating the ATP-activated current and shaping subsequent physiological responses to ATP signaling (18). Consistent with that study, blocking of  $Ca^{2+}$  influx in the present study partially inhibited ATP-induced changes in  $[Ca^{2+}]_i$ , and the P2X<sub>7</sub> agonist induced an increase in  $[Ca^{2+}]_i$ . RT-PCR analysis revealed the presence of both P2X<sub>4</sub> and P2X<sub>7</sub> receptors. Bhattacharya *et al.* suggested that the mechanisms of activation of P2X<sub>4</sub> and P2X<sub>7</sub> receptors are largely distinct, the former relying on neurotransmitter release and the latter largely on an autocrine/

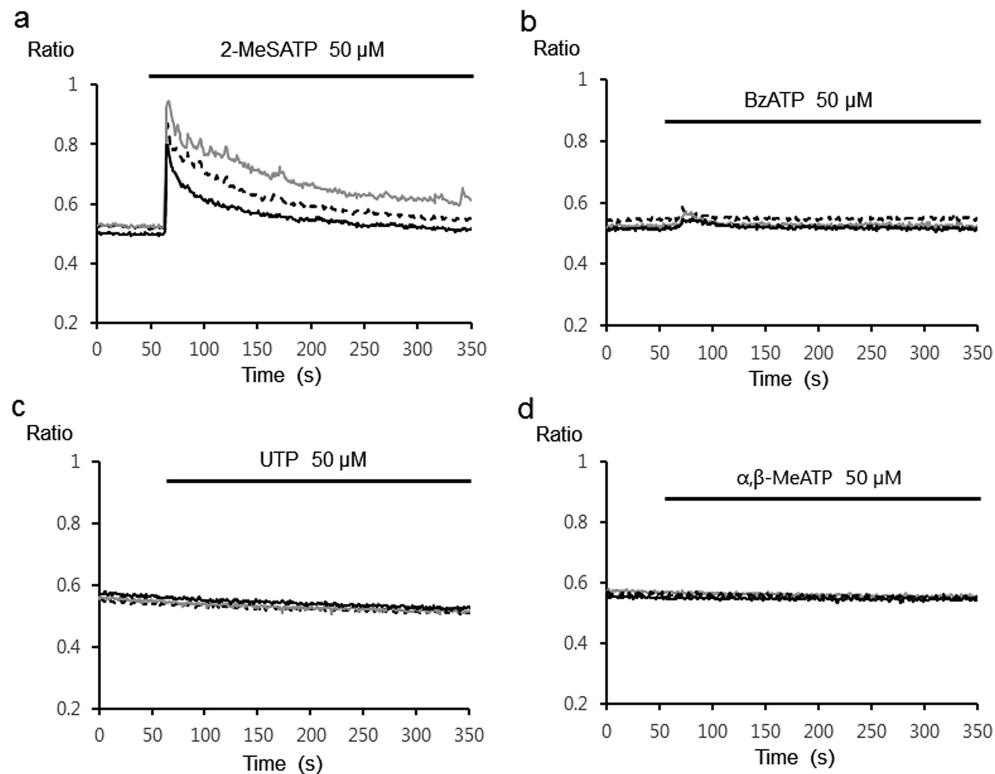


**Fig. 6** Effect of P2 purinoceptor agonists on  $[Ca^{2+}]_i$  dynamics. **a:** 2-methylthioATP (2-MeSATP), a P2Y receptor agonist (50  $\mu$ M); **b:** BzATP, a P2X<sub>7</sub> agonist (50  $\mu$ M); **c:** UTP, a P2Y<sub>2,4,6</sub> agonist (50  $\mu$ M); **d:**  $\alpha,\beta$ -methylene ATP ( $\alpha,\beta$ -MeATP), a P2X<sub>1,3</sub> agonist (50  $\mu$ M). Three ROIs were set for these analyses.

paracrine pathway (8). Li *et al.* reported that P2X<sub>7</sub> receptors require much higher concentrations of ATP for activation (millimolar concentrations) than P2Y receptors (34). However, in the present study, 50  $\mu$ M of ATP was sufficient to reproducibly induce changes in  $[Ca^{2+}]_i$  dynamics. Because ATP is present in the cytosol at concentrations around 5 mM, physical damage to cells will cause ATP to exit the cells and to move into the extracellular space, where the ATP concentration can subsequently reach 0.2–20 mM (9, 49). Accordingly, under pathological conditions, prolonged stimulation of intact cells by ATP leaked from injured cells might activate P2X<sub>7</sub>, resulting in an  $[Ca^{2+}]_i$  increase and leakage of various proteins. However, the exocytotic action of nerve endings can result in the accumulation of micromolar concentrations of extracellular ATP (26). Therefore, it is likely that the effect of ATP on parotid glands is mediated by metabotropic P2Y receptors rather than P2X receptors under physiological conditions. On the other hand, low concentrations of ATP did not stimulate amylase release, supporting the view that an increase in  $[Ca^{2+}]_i$  is not a sufficient stimulus in rat parotid gland acinar cells (59). Therefore, further studies are

necessary to elucidate the functional relation between P2Y and P2X receptors in the exocrine mechanism in parotid gland acinar cells.

Parotid gland secretion is controlled by autonomic nerves (46). Parasympathetic cholinergic stimuli elicit an IP<sub>3</sub>-dependent  $[Ca^{2+}]_i$  increase, while sympathetic adrenergic stimulation-induced  $[Ca^{2+}]_i$  dynamics are IP<sub>3</sub>-independent. We previously reported that acinar cells in exorbital lacrimal glands as well as in exocrine glands were stimulated by both cholinergic and adrenergic agonists, while myoepithelial cells responded only to cholinergic stimuli (51, 52). ATP and noradrenaline are co-stored in synaptic vesicles in sympathetic nerves. ATP-induced acinar and myoepithelial cell responses and the  $[Ca^{2+}]_i$  response of acinar cells are IP<sub>3</sub>-dependent as shown in the present study. Therefore, even under conditions of increasing in sympathetic activity, the parotid gland can both secrete saliva via an IP<sub>3</sub>-dependent mechanism and excrete fluid via myoepithelial cell contraction. It is plausible that different signaling pathways are necessary to assure that the oral surface is wet at all times. If salivation is competitively controlled by cholinergic and adrenergic nerves, it is

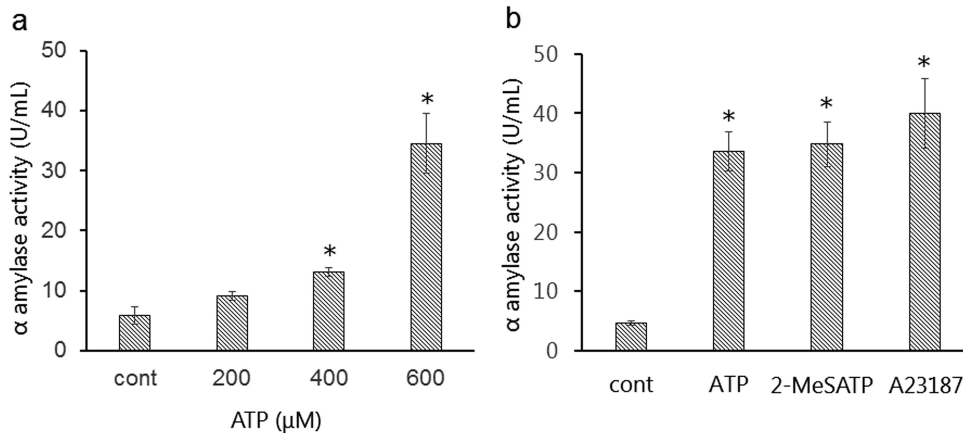


**Fig. 7** Stimulus-induced amylase release from parotid gland acinar cells. **a:** Dose-dependent effects of ATP on amylase release from mouse parotid gland acinar cells. Cells were stimulated with the indicated concentrations of ATP for 1 h. **b:** Effects of ATP on amylase release from parotid gland acinar cells. The cells were stimulated with 500 μM ATP (ATP), 500 μM 2-MeSATP (2-MeSATP), A23187 (A23187), or buffer (cont) for 1 h. Amylase activity in the supernatants was measured as described in the Materials and Methods. The data shown are the mean ± SD of three independent determinations. \* $P < 0.05$ , as determined by Student's *t*-test compared to cells without stimulation.

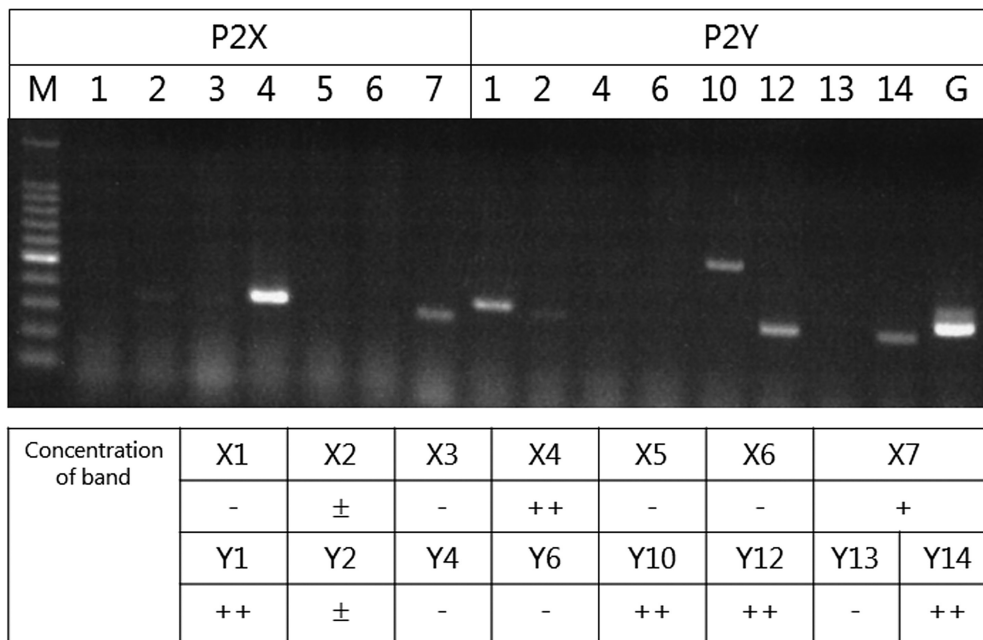


**Fig. 8** RT-PCR analysis of P2 receptor mRNA in mouse parotid gland acinar cells. P2X<sub>2,4,7</sub> and P2Y<sub>1,2,10,12,14</sub> are expressed in acinar cells. ++, very strong band on the agarose gel; +, strong and clearly visible band; ±, weak band; and -, no visible band. G, GAPDH (positive control); M, molecular standards.

possible that in certain cases, salivary secretion may be stopped, resulting in dry mouth. The present study demonstrated that stimulation with CCh and ATP induced a simultaneous increase in  $[Ca^{2+}]_i$  in most parotid acinar cells. These results are compatible with the view that stimulation of muscarinic cholinergic and purinergic receptors induces the

same signaling processes in acinar cells. Multiple studies have focused on parotid acinar cells for the production of IP<sub>3</sub> and diacylglycerol, release of Ca<sup>2+</sup> from intracellular Ca<sup>2+</sup> stores, and subsequent entry of Ca<sup>2+</sup> across the plasma membrane via a capacitative entry mechanism (5, 30, 58). The initial phase of  $[Ca^{2+}]_i$  response to a muscarinic agonist appeared

to be due to IP<sub>3</sub>-induced Ca<sup>2+</sup> release from intracellular Ca<sup>2+</sup> stores (62). Ca<sup>2+</sup> entry from the extracellular space may maintain the elevated level of [Ca<sup>2+</sup>]<sub>i</sub>, which is important for the muscarinic secretory response in acinar cells. P2Y receptors are also G-protein-coupled receptors and enhance Ca<sup>2+</sup> mobilization from intracellular Ca<sup>2+</sup> stores.

However, it remains to be resolved whether the signaling mechanism of purinergic P2Y receptors is the same as that of muscarinic receptors. In the case of lacrimal glands, our previous data showed that the direction of the intracellular Ca<sup>2+</sup> wave induced by the activation of these receptors was different; the CCh-induced wave was initiated from the luminal region (i.e., the granular region), whereas ATP elicited a Ca<sup>2+</sup> wave from the basal to the granular region (29). Differences in Ca<sup>2+</sup>-wave propagation induced by IP<sub>3</sub> and ryanodine receptors have been previously reported in pancreatic and parotid gland cells (55). At low concentrations of IP<sub>3</sub> (< 2 μM), the intracellular waves in pancreatic cells begin in the apical region and are actively propagated across the basal region by Ca<sup>2+</sup> release through ryanodine receptors. At high concentrations of IP<sub>3</sub> (> 30 μM), the waves in pancreatic and parotid cells are not true waves but rather apparent waves, formed as a result of sequential activation of IP<sub>3</sub> receptors in the apical and basal regions. Probably, the differences in wave propagation in pancreatic and parotid cells can be explained in part by differences in IP<sub>3</sub> receptor density (55). Because of the low concentrations of ATP used in the present study, further experiments are necessary to completely clarify the relationship between muscarinic and purinergic receptors in the mouse parotid gland. Regardless of the dearth of details of the intracellular signaling systems, it can be concluded that exocrine cells, especially salivary glands, possess redundant mechanisms to maintain secretion at a certain functional level.

#### Acknowledgements

We wish to express our gratitude to M. Hirakawa, Department of Anatomy, for his technical assistance. This work was supported by research grants from the Ministry of Education, Culture, Sports, Science and Technology of Japan (T.M.; 26460100, Y.S.; 15K08157) and Grants-in-Aid for Strategic Medical Science Research (S1491001, 2014-2018). Some of this work was performed at the Advanced Medical Science Center of Iwate Medical University, which also provided financial support.

The authors declare no competing financial interests.

#### REFERENCES

1. Abbracchio MP and Burnstock G (1994) Purinoceptors: Are there families of P2X and P2Y purinoceptors? *Pharmacol Ther* **64**, 445–475.
2. Abbracchio MP and Burnstock G (1998) Purinergic signaling: Pathophysiological roles. *Jpn J Pharmacol* **78**, 113–145.
3. Baker OJ, Camden JM, Ratchford AM, Seye CI, Erb L and Weisman GA (2006) Differential coupling of the P2Y1 receptor to Galpha14 and Galphaq/11 proteins during the development of the rat salivary gland. *Arch Oral Biol* **51**, 359–370.
4. Baldini C, Rossi C, Ferro F, Santini E, Seccia V, Donati V and Solini A (2013) The P2X7 receptor-inflammasome complex has a role in modulating the inflammatory response in primary Sjögren's syndrome. *J Intern Med* **274**, 480–489.
5. Baum BJ, Dai Y, Hiramatsu Y, Horn VJ and Ambudkar IS (1993) Signaling mechanisms that regulate saliva formation. *Crit Rev Oral Biol Med* **4**, 379–384.
6. Berridge MJ, Bootman MD and Roderick HL (2003) Calcium signaling: dynamics, homeostasis and remodelling. *Nat Rev Mol Cell Biol* **4**, 517–529.
7. Berridge MJ (2009) Inositol triphosphate and calcium signalling mechanisms. *Biochim Biophys Acta* **1793**, 933–940.
8. Bhattacharya S, Verrill DS, Carbone KM, Brown S, Yule DI and Giovannucci DR (2012) Distinct contributions by ionotropic purinoceptor subtypes to ATP-evoked calcium signals in mouse parotid acinar cells. *J Physiol* **590**, 2721–2737.
9. Born GV and Kratzer MA (1984) Source and concentration of extracellular adenosine triphosphate during haemostasis in rats, rabbits and man. *J Physiol* **354**, 419–429.
10. Brown DA, Bruce JI, Straub SV and Yule DI (2004) cAMP potentiates ATP-evoked calcium signaling in human parotid acinar cells. *J Biol Chem* **279**, 39485–39494.
11. Burnstock G (1972) Purinergic nerves. *Pharmacol Rev* **24**, 509–581.
12. Burnstock G (1978) A basis for distinguishing two types of purinergic receptor. In: *Cell Membrane Receptors for Drugs and Hormones: A Multidisciplinary Approach* (Straub RW and Bolis L, eds), pp 107–118, Raven Press, New York, USA.
13. Burnstock G (1995) Noradrenaline and ATP: Cotransmitters and neuromodulators. *J Physiol Pharmacol* **46**, 365–384.
14. Burnstock G (1996) P2 purinoceptors: historical perspective and classification. *Ciba Found Symp* **198**, 1–34.
15. Burnstock G (1997) The past, present and future of purine nucleotides as signalling molecules. *Neuropharmacology* **36**, 1127–1139.
16. Burnstock G (2007) Physiology and pathophysiology of purinergic neurotransmission. *Physiol Rev* **87**, 659–797.
17. Burnstock G and Knight GE (2004) Cellular distribution and functions of P2 receptor subtypes in different systems. *Int Rev Cytol* **240**, 31–304.
18. Casas-Pruneda G, Reyes JP, Pérez-Flores G, Pérez-Cornejo P and Arreola J (2009) Functional interactions between P2X4 and P2X7 receptors from mouse salivary epithelia. *J Physiol* **587**, 2887–2901.
19. Dartt DA and Hodges RR (2011) Cholinergic agonists activate P2X7 receptors to stimulate protein secretion by the rat lacrimal gland. *Invest Ophthalmol Vis Sci* **52**, 3381–3390.
20. Dartt DA and Hodges RR (2011) Interaction of {alpha}1D-adrenergic and P2X7 receptors in the rat lacrimal gland and the effect on intracellular [Ca<sup>2+</sup>] and protein secretion. *Invest Ophthalmol Vis Sci* **52**, 5720–5729.

21. Dubyak GR (1991) Signal transduction by P2-purinergic receptors for extracellular ATP. *Am J Respir Cell Mol Biol* **4**, 295–300.
22. Dubyak GR (2007) Go it alone no more—P2X7 joins the society of heteromeric ATP-gated receptor channels. *Mol Pharmacol* **72**, 1402–1405.
23. Dubyak GR and El-Moatassim C (1993) Signal transduction via P2-purinergic receptors for extracellular ATP and other nucleotides. *Am J Physiol* **265**, C577–C606.
24. Fredholm BB, Abbracchio MP, Burnstock G, Dubyak GR, Harden TK, Jacobson KA, Schwabe U and Williams M (1997) Towards a revised nomenclature for P1 and P2 receptors. *Trends Pharmacol Sci* **18**, 79–82.
25. Fujihara T, Murakami T, Fujita H, Nakamura M and Nakata K (2001) Improvement of corneal barrier function by the P2Y<sub>2</sub> agonist INS365 in a rat dry eye model. *Invest Ophthalmol Vis Sci* **42**, 96–100.
26. Gordon JL (1986) Extracellular ATP: effects, sources and fate. *Biochem J* **233**, 309–319.
27. Hodges RR, Vrovljanis J, Shatos MA and Dartt DA (2009) Characterization of P2X7 purinergic receptors and their function in rat lacrimal gland. *Invest Ophthalmol Vis Sci* **50**, 5681–5689.
28. Humphrey SP and Williamson RT (2001) A review of saliva: normal composition, flow, and function. *J Prosthet Dent* **85**, 162–169.
29. Kamada Y, Saino T, Oikawa M, Kurosaka D and Satoh Y (2012) P2Y purinoceptors induce intracellular calcium dynamics of acinar cells in rat lacrimal glands. *Histochem Cell Biol* **137**, 97–106.
30. Komabayashi T, Yakata A, Izawa T, Fujinami H, Suda K and Tsuboi M (1992) Mechanism of carbachol-stimulated diacylglycerol formation in rat parotid acinar cells. *Eur J Pharmacol* **225**, 209–216.
31. Koulen P and Thrower EC (2001) Pharmacological modulation of intracellular Ca<sup>2+</sup> channels at the single-channel level. *Mol Neurobiol* **24**, 65–86.
32. Kunapuli SP and Daniel JL (1998) P2 receptor subtypes in the cardiovascular system. *Biochem J* **336**, 513–523.
33. Leipziger J (2003) Control of epithelial transport via luminal P2 receptors. *Am J Physiol Renal Physiol* **284**, F419–F432.
34. Li Q, Luo X, Zeng W and Muallem S (2003) Cell-specific behavior of P2X7 receptors in mouse parotid acinar and duct cells. *J Biol Chem* **278**, 47554–47561.
35. Li Q, Luo X and Muallem S (2005) Regulation of the P2X7 receptor permeability to large molecules by extracellular Cl<sup>-</sup> and Na<sup>+</sup>. *J Biol Chem* **280**, 26922–26927.
36. Matsuura M, Saino T and Satoh Y (2004) Response to ATP is accompanied by a Ca<sup>2+</sup> influx via P2X purinoceptors in the coronary arterioles of golden hamsters. *Arch Histol Cytol* **67**, 95–105.
37. McConalogue K, Todorov L, Furness JB and Westfall DP (1996) Direct measurement of the release of ATP and its major metabolites from the nerve fibres of the guinea-pig taenia coli. *Clin Exp Pharmacol Physiol* **23**, 807–812.
38. Medina-Ortiz WE, Gregg EV, Brun-Zinkernagel AM and Koulen P (2007) Identification and functional distribution of intracellular ca channels in mouse lacrimal gland acinar cells. *Open Ophthalmol J* **1**, 8–16.
39. Melvin JE, Yule D, Shuttleworth T and Begenisich T (2005) Regulation of fluid and electrolyte secretion in salivary gland acinar cells. *Annu Rev Physiol* **67**, 445–469.
40. Nakamoto T, Brown DA, Catalan MA, Gonzalez-Begne M, Romanenko VG and Melvin JE (2009) Purinergic P2X7 receptors mediate ATP-induced saliva secretion by the mouse submandibular gland. *J Biol Chem* **284**, 4815–4822.
41. North RA (2002) Molecular physiology of P2X receptors. *Physiol Rev* **82**, 1013–1067.
42. Novak I (2003) ATP as a signaling molecule: the exocrine focus. *News Physiol Sci* **18**, 12–17.
43. Novak I, Jans IM and Wohlfahrt L (2010) Effect of P2X<sub>7</sub> receptor knockout on exocrine secretion of pancreas, salivary glands and lacrimal glands. *J Physiol* **588**, 3615–3627.
44. Ohtani M, Ohura K and Oka T (2011) Involvement of P2X receptors in the regulation of insulin secretion, proliferation and survival in mouse pancreatic β-cells. *Cell Physiol Biochem* **28**, 355–366.
45. Park MK, Garrad RC, Weisman GA and Turner JT (1997) Changes in P2Y1 nucleotide receptor activity during the development of rat salivary glands. *Am J Physiol* **272**, C1388–C1393.
46. Proctor GB and Carpenter GH (2007) Regulation of salivary gland function by autonomic nerves. *Auton Neurosci* **133**, 3–18.
47. Ralevic V and Burnstock G (1998) Receptors for purines and pyrimidines. *Pharmacol Rev* **50**, 413–492.
48. Reyes JP, Pérez-Cornejo P, Hernández-Carballo CY, Srivastava A, Romanenko VG, Gonzalez-Begne M, Melvin JE and Arreola J (2008) Na<sup>+</sup> modulates anion permeation and block of P2X7 receptors from mouse parotid glands. *J Membr Biol* **223**, 73–85.
49. Ryan LM, Rachow JW, McCarty BA and McCarty DJ (1996) Adenosine triphosphate levels in human plasma. *J Rheumatol* **23**, 214–219.
50. Saino T, Matsuura M and Satoh Y (2002) Comparison of the effect of ATP on intracellular calcium ion dynamics between rat testicular and cerebral arteriole smooth muscle cells. *Cell Calcium* **32**, 155–165.
51. Satoh Y, Oomori Y, Ishikawa K and Ono K (1994) Configuration of myoepithelial cells in various exocrine glands of guinea pigs. *Anat Embryol* **189**, 227–236.
52. Satoh Y, Sano K, Habara Y and Kanno T (1997) Effects of carbachol and catecholamines on ultrastructure and intracellular calcium-ion dynamics of acinar and myoepithelial cells of lacrimal glands. *Cell Tissue Res* **289**, 473–485.
53. Schwiebert EM and Zsembery A (2003) Extracellular ATP as a signaling molecule for epithelial cells. *Biochim Biophys Acta* **1615**, 7–32.
54. Segawa A, Takemura H and Yamashina S (2002) Calcium signalling in tissue: diversity and domain-specific integration of individual cell response in salivary glands. *J Cell Sci* **115**, 1869–1876.
55. Sneyd J, Tsaneva-Atanasova K, Bruce JI, Straub SV, Giovannucci DR and Yule DI (2003) A model of calcium waves in pancreatic and parotid acinar cells. *Biophys J* **85**, 1392–1405.
56. Soltoff SP, McMillian MK, Lechleiter JD, Cantley LC and Talamo BR (1990) Elevation of [Ca<sup>2+</sup>]<sub>i</sub> and the activation of ion channels and fluxes by extracellular ATP and phospholipase C-linked agonists in rat parotid acinar cells. *Ann N Y Acad Sci* **603**, 76–90.
57. Surprenant A, Rassendren F, Kawashima E, North RA and Buell G (1996) The cytolytic P2Z receptor for extracellular ATP identified as a P2X receptor (P2X<sub>7</sub>). *Science* **272**, 735–738.
58. Takemura H and Putney JW Jr (1989) Capacitative calcium entry in parotid acinar cells. *Biochem J* **258**, 409–412.
59. Tojyo Y, Tanimura A, Matsui S and Matsumoto Y (1997) Ef-

- fects of extracellular ATP on cytosolic  $\text{Ca}^{2+}$  concentration and secretory responses in rat parotid acinar cells. *Arch Oral Biol* **42**, 393–399.
60. von Kügelgen I and Starke K (1991) Noradrenaline-ATP co-transmission in the sympathetic nervous system. *Trends Pharmacol Sci* **12**, 319–324.
61. Yang J, McBride S, Mak DO, Vardi N, Palczewski K, Haeseleer F and Foskett JK (2002) Identification of a family of calcium sensors as protein ligands of inositol trisphosphate receptor  $\text{Ca}^{2+}$  release channels. *Proc Natl Acad Sci U S A* **99**, 7711–7716.
62. Zhang GH and Melvin JE (1993) Membrane potential regulates  $\text{Ca}^{2+}$  uptake and inositol phosphate generation in rat sublingual mucous acini. *Cell Calcium* **14**, 551–562.
63. Zhang Z, Wang Z, Ren H, Yue M, Huang K, Gu H, Liu M, Du B and Qian M (2011)  $\text{P2Y}_6$  agonist uridine 5'-diphosphate promotes host defense against bacterial infection via monocyte chemoattractant protein-1-mediated monocytes/macrophages recruitment. *J Immunol* **186**, 5376–5387.